

Oxygen Uptake Rates and Liver-Specific Functions of Hepatocyte and 3T3 Fibroblast Co-Cultures

Cheul H. Cho, Jaesung Park, Deepak Nagrath, Arno W. Tilles, François Berthiaume, Mehmet Toner, Martin L. Yarmush

Center for Engineering in Medicine and Department of Surgery, Massachusetts General Hospital, Harvard Medical School, and the Shriners Hospitals for Children, 51 Blossom St, Boston, Massachusetts 02114; telephone: 617-371-4882; fax: 617-371-4950; e-mail: ireis@sbi.org

Received 30 April 2006; accepted 20 September 2006

Published online 19 October 2006 in Wiley InterScience (www.interscience.wiley.com). DOI 10.1002/bit.21225

ABSTRACT: Bioartificial liver (BAL) devices have been developed to treat patients undergoing acute liver failure. One of the most important parameters to consider in designing these devices is the oxygen consumption rate of the seeded hepatocytes which are known to have oxygen consumption rates 10 times higher than most other cell types. Hepatocytes in various culture configurations have been tested in BAL devices including those formats that involve co-culture of hepatocytes with other cell types. In this study, we investigated, for the first time, oxygen uptake rates (OURs) of hepatocytes co-cultured with 3T3-J2 fibroblasts at various hepatocyte to fibroblast seeding ratios. OURs were determined by measuring the rate of oxygen disappearance using a ruthenium-coated optical probe after closing and sealing the culture dish. Albumin and urea production rates were measured to assess hepatocyte function. Lower hepatocyte density co-cultures demonstrated significantly higher OURs (2 to 3.5-fold) and liver-specific functions (1.6-fold for albumin and 4.5-fold for urea production) on a per cell basis than those seeded at higher densities. Increases in OUR correlated well with increased liver-specific functions. OURs (V_m) were modeled by fitting Michaelis–Menten kinetics and the model predictions closely correlated with the experimental data. This study provides useful information for predicting BAL design parameters that will avoid oxygen limitations, as well as maximize metabolic functions.

Biotechnol. Bioeng. 2007;97: 188–199.

© 2006 Wiley Periodicals, Inc.

KEYWORDS: oxygen uptake rate; hepatocyte; co-culture; seeding density; mathematical modeling

Introduction

Orthotopic liver transplantation is an effective treatment for end-stage liver disease. However, due to the severe shortage of donors, many patients with acute liver failure die while waiting for a donor liver. The extracorporeal bioartificial liver (BAL) device is a promising therapeutic modality that could provide temporary support for patients with liver failure until an organ is available or until the patient's native liver regenerates. Although most clinical trials of BAL devices have used designs that incorporate hollow-fiber technology, it has been suggested that these devices are subject to oxygen and substrate limitations that could result in reduced hepatocyte viability and function (Catapano, 1996; Hay et al., 2000), and therefore, could account for their limited therapeutic efficacy (Demetriou et al., 2004; Ellis et al., 1996). Cultured hepatocytes exhibit very high oxygen uptake rates (OURs) (Balis et al., 1999; Foy et al., 1994; Rotem et al., 1992; Shatford et al., 1992; Smith et al., 1996), and adequate oxygen delivery to the hepatocytes is imperative for their ability to maintain stable liver-specific functions. As a means of supplying adequate oxygenation to the hepatocytes in a BAL device, designs that have incorporated membrane oxygenators have demonstrated improved bioreactor performance (De Bartolo et al., 2000; Peng and Palsson, 1996; Shito et al., 2003; Tilles et al., 2001a).

It has previously been reported that hepatocytes co-cultured with other cell types improve hepatocyte function and life span in culture (Bhatia et al., 1999; Fraslín et al., 1985; Guguen-Guillouzo et al., 1983), whereas

Correspondence to: M.L. Yarmush

Contract grant sponsor: NIH

Contract grant numbers: DK43371; DK59766; DK66040; EB002503

Contract grant sponsor: Shriners Hospitals for Children

 WILEY
InterScience®
DISCOVER SOMETHING GREAT

primary hepatocytes cultured alone lose their characteristic morphology and function. In co-culture systems, heterotypic cell–cell contact plays an important role for the maintenance of liver-specific function (Bhatia et al., 1998; Mesnil et al., 1987). Hepatocyte function varies depending on the seeding ratio of hepatocytes and other cell types. BAL devices with co-culture systems have been employed to maintain stable liver-specific functions (Park et al., 2005; Tilles et al., 2001b). Although OURs of hepatocytes have been measured when cultured alone in various culture configurations, such as in 3-D gels (Nyberg et al., 1993, 1994; Sielaff et al., 1997), on microcarriers (Smith et al., 1996), and in monolayers (Balis et al., 1999; Foy et al., 1994; Rotem et al., 1992; Yarmush et al., 1992), no studies have reported on OURs of hepatocytes for various seeding ratios in co-culture systems.

In this study, to evaluate the effect of seeding parameters on OUR and the expression of liver-specific functions, isolated rat hepatocytes were co-cultured with fibroblasts (3T3-J2) at hepatocyte to fibroblast ratios of 1 to 9 (low hepatocyte density), 1 to 3 (medium hepatocyte density), and 9 to 1 (high hepatocyte density), while keeping the initial number of total cells seeded per dish constant. There was an inverse relationship between the hepatocyte density and OURs of hepatocytes in co-culture. Hepatocytes seeded at lower densities in co-culture demonstrated significantly higher OURs compared to those seeded at higher densities. The increased OUR correlated well with increased liver-specific functions. The measured OURs for the co-cultures were higher than those calculated by linear summation of OURs of individual cell types. Hence, OURs (V_m) were modeled by fitting Michaelis–Menten kinetics to predict the experimental data measured in the co-culture system. The predictions by a nonlinear Michaelis–Menten based model closely correlated with the experimental data. The results obtained in this study may be useful in the design of BAL devices.

Materials and Methods

Materials

Hepatocyte culture medium consisted of DMEM supplemented with 10% fetal bovine serum (Gibco, Gaithersburgh,

MD), 7 ng/mL glucagon (Bedford Laboratories, Bedford, OH), 7.5 μ g/mL hydrocortisone (Pharmacia Corporation, Kalamazoo, MI), 0.5 U/mL insulin (Eli Lilly, Indianapolis, IN), 20 ng/mL epidermal growth factor (Sigma Chemical Co., St. Louis, MO), 200 U/mL penicillin, and 200 μ g/mL streptomycin (Gibco).

Hepatocyte Isolation and Culture

Hepatocytes were isolated from adult female Lewis rats (Charles River Laboratories, Boston, MA) weighing 150–200 g, using a two-step collagenase perfusion procedure modified from Seglen (1976) as described previously (Berthiaume et al., 1996; Dunn et al., 1991, 1992). Typically, 200–300 million hepatocytes were obtained with viability >90% as determined by trypan blue exclusion. Tissue culture dishes (60 mm, surface area of 21 cm²) were coated with a solution of type I rat tail collagen (0.11 mg/mL) for 30 min at 37°C. After rinsing the dishes twice with PBS, hepatocytes were seeded at three different densities (Table I) in 2 mL hepatocyte culture medium, and kept in 90% air/10% CO₂ at 37°C. To achieve uniform cell distribution, the substrates were shaken every 15 min for the first hour after cell seeding. The following day, after aspirating the hepatocyte culture medium from the dishes, 3T3-J2 fibroblasts were seeded at three different densities, for a total initial cell number (hepatocytes + fibroblasts) of 2×10^6 cells/60-mm dish, giving initial hepatocyte to fibroblast ratios of 1 to 9 (low hepatocyte density), 1 to 3 (medium hepatocyte density), and 9 to 1 (high hepatocyte density) (Table I). The next day, the fibroblast medium was aspirated, and 2 mL of hepatocyte culture medium was applied to each dish. Culture medium was changed daily and samples were stored at 4°C for biological functional analysis. OURs were measured 2, 7, 10, and 14 days after hepatocyte seeding. The OURs of pure hepatocyte and fibroblast cultures were also measured as controls. For OUR measurement in pure hepatocyte cultures, 2 million hepatocytes were seeded in 2 mL culture medium. OURs of pure hepatocytes were measured on post-seeding day 1 to compare with previously published values (Foy et al., 1994). To measure OURs of pure hepatocytes in stable long-term cultures, 2 million hepatocytes were seeded and cultured in

Table I. Initial seeding ratios of hepatocytes and fibroblasts in co-cultures.

Hepatocyte:fibroblast ratio	No. of hepatocytes	No. of fibroblasts	No. of total cells
H:F = 1:9	$0.2 \times 10^6/60\text{-mm dish}$ ($9.52 \times 10^3/\text{cm}^2$)	$1.8 \times 10^6/60\text{-mm dish}$ ($85.70 \times 10^3/\text{cm}^2$)	$2.0 \times 10^6/60\text{-mm dish}$ ($95.24 \times 10^3/\text{cm}^2$)
H:F = 1:3	$0.5 \times 10^6/60\text{-mm dish}$ ($23.81 \times 10^3/\text{cm}^2$)	$1.5 \times 10^6/60\text{-mm dish}$ ($71.43 \times 10^3/\text{cm}^2$)	$2.0 \times 10^6/60\text{-mm dish}$ ($95.24 \times 10^3/\text{cm}^2$)
H:F = 9:1	$1.8 \times 10^6/60\text{-mm dish}$ ($85.70 \times 10^3/\text{cm}^2$)	$0.2 \times 10^6/60\text{-mm dish}$ ($9.52 \times 10^3/\text{cm}^2$)	$2.0 \times 10^6/60\text{-mm dish}$ ($95.24 \times 10^3/\text{cm}^2$)

The surface area of 60-mm dish is 21 cm².

the collagen gel sandwich configuration (Dunn et al., 1989) and OURs were measured after 14 days of culture. To measure OURs of pure fibroblasts, 2 million fibroblasts were seeded in 2 mL culture medium and were measured 0, 3, 4, and 13 days after seeding. The fibroblast cell numbers on each day were counted using a hemacytometer after trypsinizing the cells. OURs of pure hepatocytes and fibroblasts were normalized to cell number and expressed as nmol/s/10⁶ cells. Murine 3T3-J2 fibroblasts (purchased from Howard Green, Harvard Medical School, Boston, MA) were maintained in T175 tissue culture flasks in DMEM (Gibco) plus 10% FBS and 2% penicillin and streptomycin prior to seeding.

Oxygen Uptake Rate Measurement Device and Technique

OURs of co-cultured hepatocytes and fibroblasts were measured using a device described by Rotem et al. (1992) and Foy et al. (1994). Briefly, the device consisted of a polycarbonate disc machined to fit onto a 60-mm tissue culture dish (Fig. 1). When the device was placed on the tissue culture dish, an airtight seal was obtained by using vacuum grease at the interface of the culture dish and the device. A variable speed electric motor turned a magnetic stir bar at a constant speed of 1,800 rpm to ensure uniform mixing of the medium within the dish. Oxygen tension in the culture was measured with a ruthenium-coated optical probe (Ocean Optics, Dunedin, FL), which used the fluorescence of a ruthenium complex in a sol-gel matrix that is sensitive to partial oxygen pressure (Krihak and Shahriari, 1996). Oxygen tension data were collected via a USB interface card connected to a PC computer equipped with signal processing software. Since it was a closed system during the oxygen tension measurement, the change in oxygen concentration versus time reflects oxygen uptake by

the cells. We assumed Michaelis–Menten kinetics for oxygen uptake and fitted the experimental data to the equation:

$$\frac{dP}{dt} = \frac{-V_m P}{K_{0.5} + P} \left(\frac{N_c}{kV} \right) \quad (1)$$

where P is the measured oxygen partial pressure (mmHg), t is time (s), N_c is the number of cells in the device chamber, k is the solubility of oxygen in water at 37°C (1.19 nmol/mL-mmHg), and V is the liquid volume in the device chamber (11.5 mL). Prior to OUR measurement, a calibration was performed using 21 and 0% oxygen tension standards. The 21% oxygen standard was prepared by incubating PBS in a 21% oxygen atmosphere at 37°C for 2 h. The 0% oxygen standard was prepared by adding saturating amounts of sodium hydrosulfite (~20%) into pre-warmed de-ionized water at 37°C. Calibration was repeated and the oxygen tension measured in this second set of standards was identical to the first set. Oxygen sensor calibration using the first set of standards was performed before each measurement to compensate for drift of the sensor. Following the calibration, the culture medium was removed from the cell culture dish and replaced with medium equilibrated in 90% air/10% CO₂ at 37°C before the measurement. The oxygen measurement device was assembled with the tissue culture dish and the oxygen partial pressure versus time was recorded. Oxygen uptake parameters (V_m and $K_{0.5}$) were computationally generated from the oxygen partial pressure versus time curve. The $K_{0.5}$ values were determined by computing the slope of oxygen partial pressure versus time curve at which the OUR is half-maximal of V_m .

Albumin and Urea Assays

The collected culture medium was analyzed for rat serum albumin content by enzyme-linked immunosorbent assay

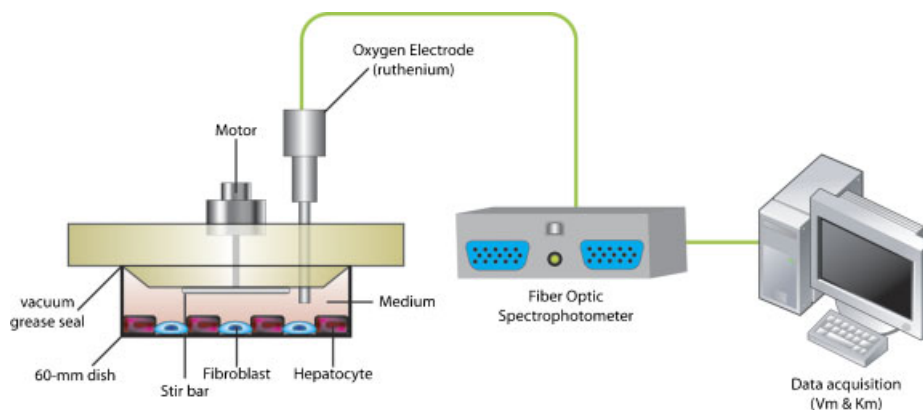


Figure 1. Schematic diagram of oxygen measurement device.

(ELISA) with purified rat albumin and a peroxidase-conjugated antibody (MP Biomedicals, Aurora, OH). Urea content was determined with a commercially available kit (StanBio Laboratory, Boerne, TX). Standard curves were generated using purified rat albumin or urea dissolved in culture medium. Absorbances were measured with a Thermomax microplate reader (Molecular Devices, Sunnyvale, CA).

Immunofluorescent Staining

The in situ immunofluorescence staining of albumin was visualized with fluorescein isothiocyanate (FITC) to track hepatocytes in co-cultures. For intracellular albumin staining of hepatocytes, cultures in 60-mm tissue culture dishes were washed twice with phosphate-buffered saline (PBS) and fixed in 2% paraformaldehyde in PBS at room temperature for 20 min. After incubation, the dishes were washed twice in PBS, followed by adding 0.2% Triton X-100 in PBS to permeabilize cells for intracellular staining. After 5 min incubation at room temperature, the cells were washed twice in PBS and incubated in PBS/20% FBS/0.1% Triton/0.5% DMSO for 60 min at room temperature to block nonspecific antibody binding. After incubation, the primary antibody, goat IgG to rat albumin (MP Biomedicals, Aurora, OH), was added and incubated for 60 min at room temperature. After washing twice in blocking solution, the cells were incubated with the secondary antibody FITC-conjugated rabbit IgG to goat IgG (MP Biomedicals, Aurora, OH), for 60 min at room temperature, and washed twice at room temperature. Cells were counterstained with 4,6-diamidino-2-phenylindole (DAPI) for nuclear staining to count number of cell nuclei and were visualized by fluorescence microscopy (Zeiss, Thornwood, NY).

Cell Counting

For each culture condition tested, duplicate dishes were sacrificed on days 2, 7, 10, and 14 for analysis. Cultures were stained with FITC for intracellular albumin and DAPI nuclear staining and visualized by fluorescence microscopy (100× objective). In one field, cells positively stained for albumin (corresponding to hepatocytes) were manually counted. Individual hepatocytes could be easily distinguished as membrane borders were clearly visible. A multinucleated hepatocyte was counted as a single cell. To determine fibroblast numbers, first the total number of DAPI stained nuclei per field was counted using an automated tool in Metamorph image analysis software (Universal Imaging, Westchester, PA). Then, the number of hepatocyte nuclei (in the albumin-positive regions of the culture) were manually counted and subtracted from the total number of nuclei. The result, corresponding to the number of fibroblast nuclei, was used as an estimate of fibroblast number, as fibroblasts are rarely found multinucleated. Four to six fields were analyzed among duplicate

culture dishes, and the results averaged. The numbers of counted cells per field were normalized to the values determined on day 2. To convert to cell numbers per dish, the normalized values were multiplied by the known number of seeded cells. This procedure was justified as the cell numbers on day 2 were experimentally found to be within 90% of the number of seeded cells.

Mathematical Modeling

To predict OURs (V_m) in co-culture systems, we developed a nonlinear Michaelis–Menten based model:

$$\text{OUR}(V_{m,\text{coculture}}) = \frac{(aV_{m,\text{hep}}N_{\text{hep}})t}{1 + (cV_{m,\text{hep}}N_{\text{hep}} + dV_{m,\text{fb}}N_{\text{fb}})t} + \frac{(bV_{m,\text{fb}}N_{\text{fb}})t}{1 + (eV_{m,\text{hep}}N_{\text{hep}} + fV_{m,\text{fb}}N_{\text{fb}})t} \quad (2)$$

where $V_{m,\text{coculture}}$ denotes OURs in co-culture (nmol/s/60-mm dish); $V_{m,\text{hep}}$ denotes OUR of pure hepatocytes (nmol/s/10⁶ hepatocytes), $V_{m,\text{fb}}$ denotes OUR of pure fibroblasts (nmol/s/10⁶ fibroblasts); N_{hep} denotes the hepatocyte number ($\times 10^6$ cells); N_{fb} denotes the fibroblast cell number ($\times 10^6$ cells); and t denotes time (days). The parameters a – f were calculated by constrained nonlinear optimization using MATLAB. We used training data (OUR for days, 2, 7, and 10) to optimize the parameters a – f . Day 14 data set was treated as test or validation data set and was never used to generate the model parameters. Linear summation of OURs, where OURs for co-culture were the sum of OURs of individual cell types ($V_{m,\text{coculture}} = V_{m,\text{hep}}N_{\text{hep}} + V_{m,\text{fb}}N_{\text{fb}}$), was also tested and compared with the experimental data measured for the co-cultures.

Statistical Analysis

Results are expressed as mean \pm standard deviation (SD). Statistical analysis on OUR (V_m) and liver-specific functions (albumin and urea) was performed by a two-tailed unpaired student's t -test. Probability values less than 0.05 were considered statistically significant.

Results

Oxygen Uptake Rates (OURs) of Hepatocyte and Fibroblast Co-Cultures

The objective of this experiment was to examine OURs of hepatocyte and fibroblast co-cultures at various seeding ratios and to understand the effect of hepatocyte seeding density on OURs and liver-specific functions. OURs at three ratios of hepatocytes to fibroblasts (1:9, 1:3, and 9:1) were measured 2, 7, 10, and 14 days after seeding. Figure 2 shows a

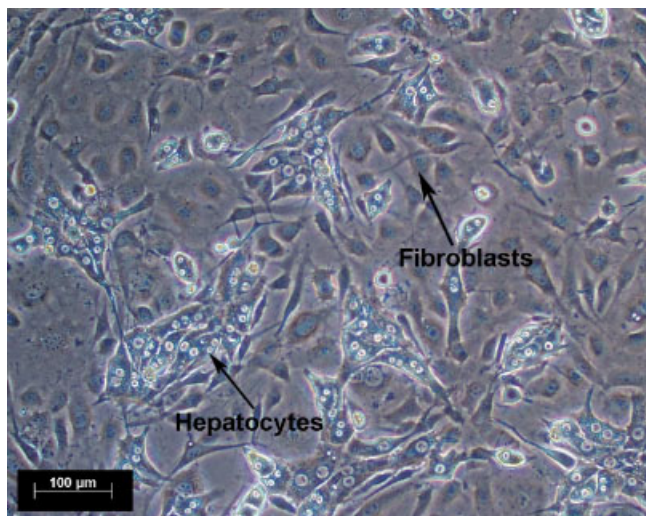


Figure 2. Phase-contrast image of co-cultures 2 days after seeding (H:F = 1:3). Scale bar, 100 μm .

phase contrast image of a co-culture having an initial hepatocyte to fibroblast ratio of 1 to 3 (H:F = 1:3).

As controls, OURs of fibroblast ($V_{m,fb}$) and hepatocyte ($V_{m,hep}$) monocultures were measured to evaluate the actual contribution of hepatocytes to the OURs in the co-culture system. Monocultures of hepatocytes in the early phase of culture (day 1) consumed $\sim 38\%$ more oxygen (0.33 ± 0.03 nmol/s/ 10^6 hepatocytes, $n = 5$) than those in stable long-term cultures in the collagen gel sandwich configuration at day 14 (0.24 ± 0.02 nmol/s/ 10^6 hepatocytes, $n = 3$). The value on day 1 was in good agreement with previously published data (0.38 ± 0.12 nmol/s/ 10^6 hepatocytes, $n = 4$) by Foy et al. (1994). A much lower OUR (0.06 ± 0.02 nmol/s/ 10^6 fibroblasts, $n = 4$) was measured for monocultures of fibroblasts, and this value was constant over the culture time period (days 0, 3, 4, and 13). Compared to fibroblasts, OURs of hepatocytes were approximately 4–5.5 times higher. Cell numbers in the co-culture systems, determined by counting cell nuclei, increased continuously through day

14 (Table II). Initial total cell numbers in co-culture (total 2×10^6 cells/60-mm dish) had increased about 1.8 times by day 14. Hepatocyte numbers in high, medium, and low hepatocyte density cultures increased by approximately 1.4-, 2-, and 3-fold over 14 days, respectively. Lower hepatocyte density co-cultures demonstrated greater hepatocyte proliferation than those at higher densities.

For the hepatocyte/fibroblast co-cultures, the OURs ($V_{m,max}$) per dish (surface area of 21 cm^2) increased over time and reached a plateau on culture day 10 for the three hepatocyte to fibroblast ratios tested (Fig. 3A). Among the three ratios, the OUR on each day was greatest for the high hepatocyte density co-culture. The OURs per unit surface area (21 cm^2) for the H:F ratios of 9:1, 1:3, and 1:9 at day 10 were 0.74, 0.62, and 0.49 nmol/s/60-mm dish, respectively, indicating relatively high oxygen consumption per unit surface area occurs at lower hepatocyte densities (H:F = 1:3 and 1:9) considering that the initial number of seeded hepatocytes were fourfold and ninefold lower, respectively, than at the high hepatocyte density (H:F = 9:1). To determine the effect of hepatocyte density in co-culture on hepatocyte OUR, the OURs of hepatocytes in co-culture were calculated by subtracting the OURs of fibroblasts alone ($V_{m,fb} \times \text{No. of fibroblasts}$) from the measured OURs of hepatocyte and fibroblast co-cultures ($V_{m,co-culture}$), and then normalizing to the hepatocyte number (Fig. 3B). Hepatocyte OURs on days 2, 7, 10, and 14 at the low (H:F = 1:9) and medium (H:F = 1:3) hepatocyte densities were significantly higher than those at high (H:F = 9:1) hepatocyte density. The OURs at the low hepatocyte density (H:F = 1:9) were ~ 2.5 times higher on day 2, ~ 3.5 times higher on day 7, and ~ 2 times higher on days 10 and 14, compared to those at the corresponding high hepatocyte density (H:F = 9:1). The OUR for the low hepatocyte density co-cultures peaked on day 7, and progressively declined on days 10 and 14. The OURs at the medium and high hepatocyte densities remained relatively constant throughout the culture period. Figure 4 shows the correlation between hepatocyte seeding densities and the OURs of hepatocytes in co-culture. In early (day 2) and late (day 10) stages of culture, there was an inverse relationship between the hepatocyte density and the OURs of hepatocytes in co-culture. As the hepatocyte

Table II. Cell numbers ($\times 10^6$ cells) in hepatocyte and fibroblast co-cultures.

Days	H:F = 1:9		H:F = 1:3		H:F = 9:1	
	#Hep	#Fb	#Hep	#Fb	#Hep	#Fb
2	0.20 ± 0.00	1.80 ± 0.00	0.50 ± 0.00	1.50 ± 0.00	1.80 ± 0.00	0.20 ± 0.00
7	0.34 ± 0.06	2.26 ± 0.16	0.97 ± 0.05	2.18 ± 0.08	2.12 ± 0.12	0.53 ± 0.06
10	0.53 ± 0.10	2.64 ± 0.09	0.91 ± 0.12	2.26 ± 0.09	2.31 ± 0.09	0.85 ± 0.05
14	0.57 ± 0.08	2.77 ± 0.11	0.99 ± 0.11	2.35 ± 0.15	2.49 ± 0.15	1.13 ± 0.08

Cell numbers were determined by counting cell nuclei and normalized to initial cell number as described in the Materials and Methods section. It was assumed that cell numbers on day 2 were the same as initial cell numbers since cell numbers counted by hemacytometer after trypsin treatment on day 2 were close to initial seeding cell numbers ($>90\%$). Data are expressed as means \pm standard deviations.

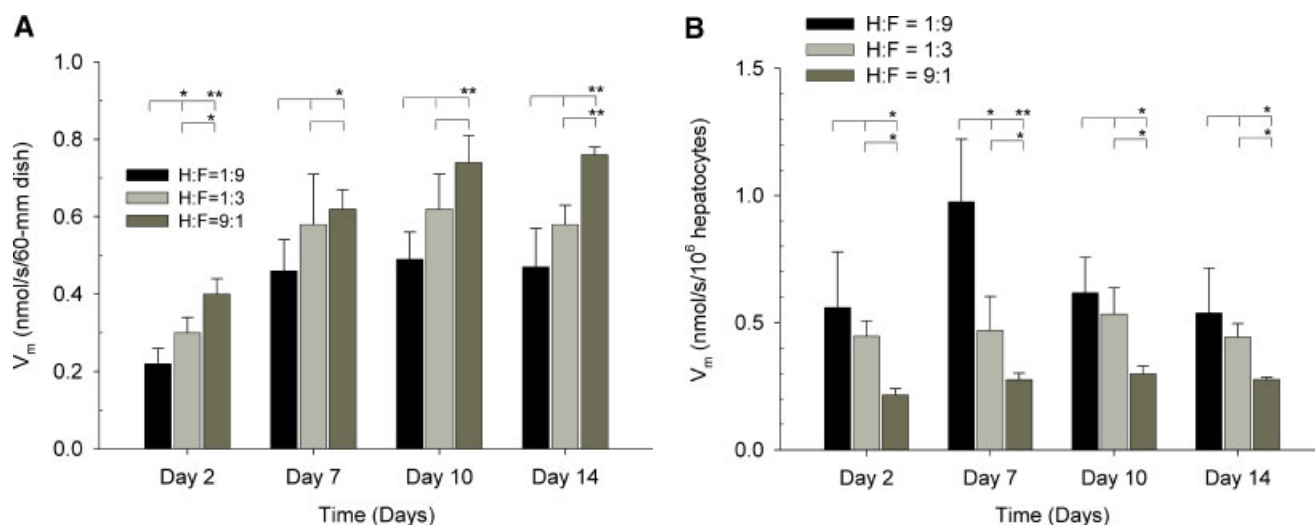


Figure 3. Maximal OUR (V_m) values of hepatocyte and fibroblast co-cultures. **A:** OURs of total cells per 60-mm dish (surface area = 21 cm²). **B:** OURs of hepatocytes normalized to hepatocyte numbers (nmol/s/ 10^6 hepatocytes). OURs of hepatocytes per dish in co-cultures were obtained after subtracting the OURs of total fibroblasts, and then normalized to hepatocyte numbers. Data shown are means \pm standard deviations (SD) of three independent experiments ($n=3-5$). * $P < 0.05$; ** $P < 0.005$.

density increased, the OURs of hepatocytes in co-culture decreased. These results show that lower seeding densities of hepatocytes in co-cultures have significantly higher OURs than those seeded at higher densities. The OURs began to decline when the oxygen partial pressure dropped below approximately 10–15 mmHg. The estimated $K_{0.5}$ values remained constant during the 14-day culture period. Lower seeding densities of hepatocytes tended to have slightly higher $K_{0.5}$ values than those for higher seeding densities both on days 10 and 14 (data not shown).

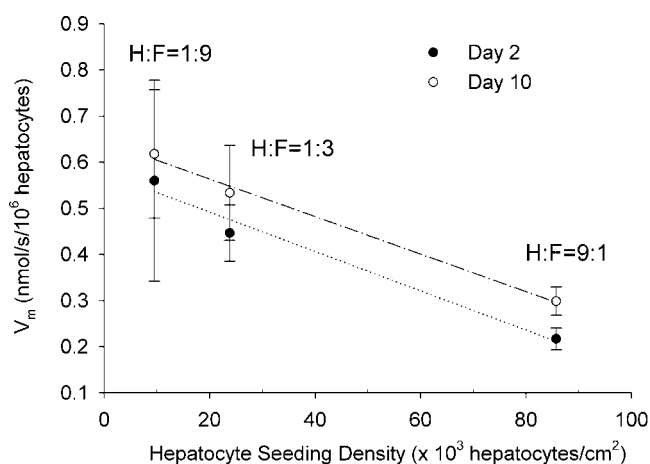


Figure 4. Effect of hepatocyte seeding density on OUR (V_m) in early (day 2) and late (day 10) stages of culture. Data shown are means \pm standard deviations of three independent experiments ($n=3-5$).

Hepatocyte Functions

Liver specific functions (e.g., albumin and urea synthesis rates) were measured for the co-cultures at three different hepatocyte-to-fibroblast ratios. The albumin secretion rates of hepatocytes co-cultured with fibroblasts progressively increased through culture day 10 for all three hepatocyte-to-fibroblast ratios (Fig. 5A). On day 10, albumin secretion rates per 60-mm culture dish were approximately 167 μ g/day for high density (H:F = 9:1), 100 μ g/day for medium density (H:F = 1:3), and 62 μ g/day for low density (H:F = 1:9) hepatocyte co-cultures. The high density hepatocyte co-cultures (H:F = 9:1), which initially had nine times more hepatocytes per dish than low hepatocyte density co-cultures (H:F = 1:9), exhibited ~ 2.7 times higher albumin secretion per dish than the low density co-cultures. In contrast, when the albumin secretion rates were normalized to the number of hepatocytes per dish, as determined by cell nuclei counting, the low (H:F = 1:9) and medium (H:F = 1:3) hepatocyte densities co-cultures demonstrated higher albumin secretion rates on a per hepatocyte basis than those culture seeded at high (H:F = 9:1) hepatocyte density (Fig. 5B). The albumin secretion rate per 1×10^6 hepatocytes on day 10 was approximately 116 μ g/day for low density (H:F = 1:9), 109 μ g/day for medium density (H:F = 1:3), and 73 μ g/day for high density (H:F = 9:1) hepatocyte co-cultures. In general, the urea synthesis rates per dish of hepatocytes co-cultured with fibroblasts progressively increased through culture day 10 for all three hepatocyte seeding densities (Fig. 6A). There were no significant differences in the urea synthesis rates for the three hepatocyte seeding densities on days 10 and 14. In contrast, when normalized to the number

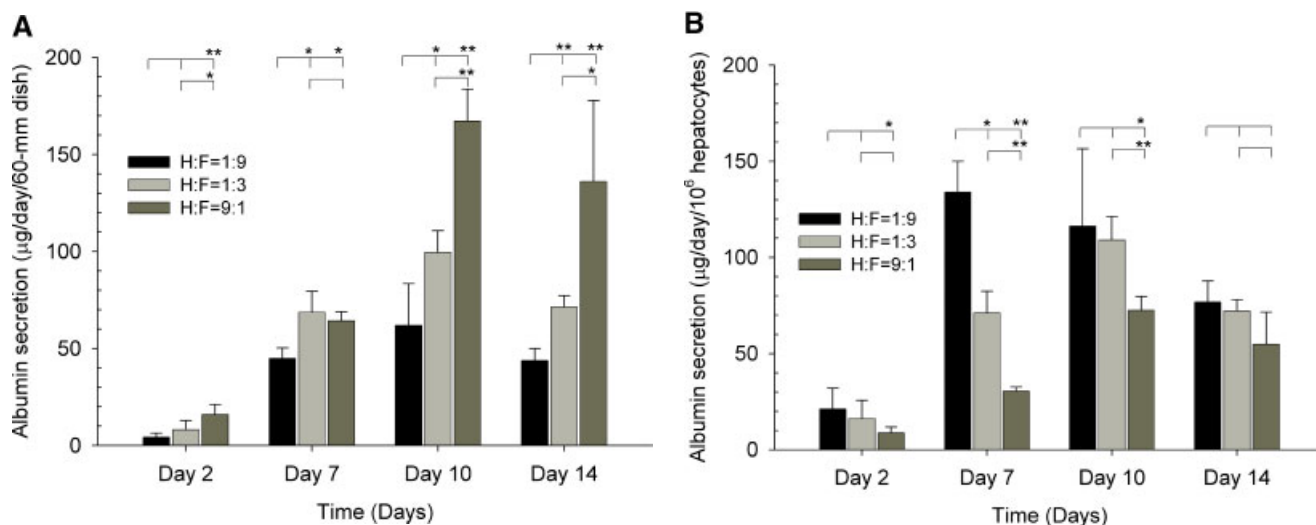


Figure 5. Albumin secretion of hepatocyte and fibroblast co-cultures. **A:** Albumin secretion per 60-mm dish ($\mu\text{g}/\text{day}/60\text{-mm dish}$). **B:** Albumin secretion normalized to hepatocyte number ($\mu\text{g}/\text{day}/10^6$ hepatocytes) on days 2, 7, 10, and 14. Data shown are means \pm standard deviations of three different experiments ($n = 5-7$). * $P < 0.05$; ** $P < 0.005$.

of hepatocytes per dish, the urea synthesis rates were significantly higher for the low density hepatocyte co-cultures compared to the medium and high density hepatocyte co-cultures (Fig. 6B). The urea synthesis rate for low density (H:F = 1:9) hepatocyte co-cultures on day 10 was approximately 4.5-fold and 1.6-fold higher than those for high density (H:F = 9:1) and medium density (H:F = 1:3) hepatocyte co-cultures on day 10, respectively. The urea synthesis rates for the medium density hepatocyte co-cultures were also significantly higher than the high-density co-cultures.

Correlation Between Oxygen Consumption Rates and Liver-Specific Functions

Figure 7 shows the relationship between the liver specific functions of the hepatocyte/fibroblast co-cultures, for the three hepatocyte seeding densities, and their OURs. In early (day 2) and late (day 10) stages of culture, there was a linear relationship between albumin secretion rates or urea synthesis rates and OURs. Similar trends were also observed on days 7 and 14. In all cases, for lower hepatocyte seeding density co-cultures, there was increased albumin and urea

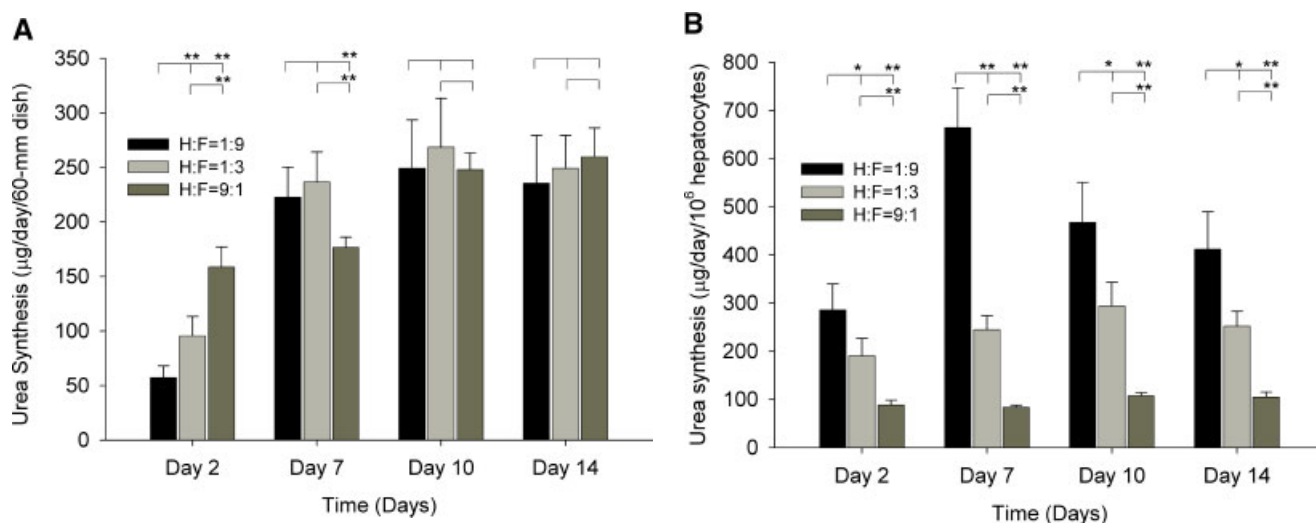


Figure 6. Urea synthesis of hepatocyte and fibroblast co-cultures. **A:** Urea synthesis per 60-mm dish ($\mu\text{g}/\text{day}/60\text{-mm dish}$). **B:** Urea synthesis normalized to hepatocyte numbers ($\mu\text{g}/\text{day}/10^6$ hepatocytes) on days 2, 7, 10, and 14. Data shown are means \pm standard deviations of three different experiments ($n = 5-7$). * $P < 0.05$; ** $P < 0.005$.

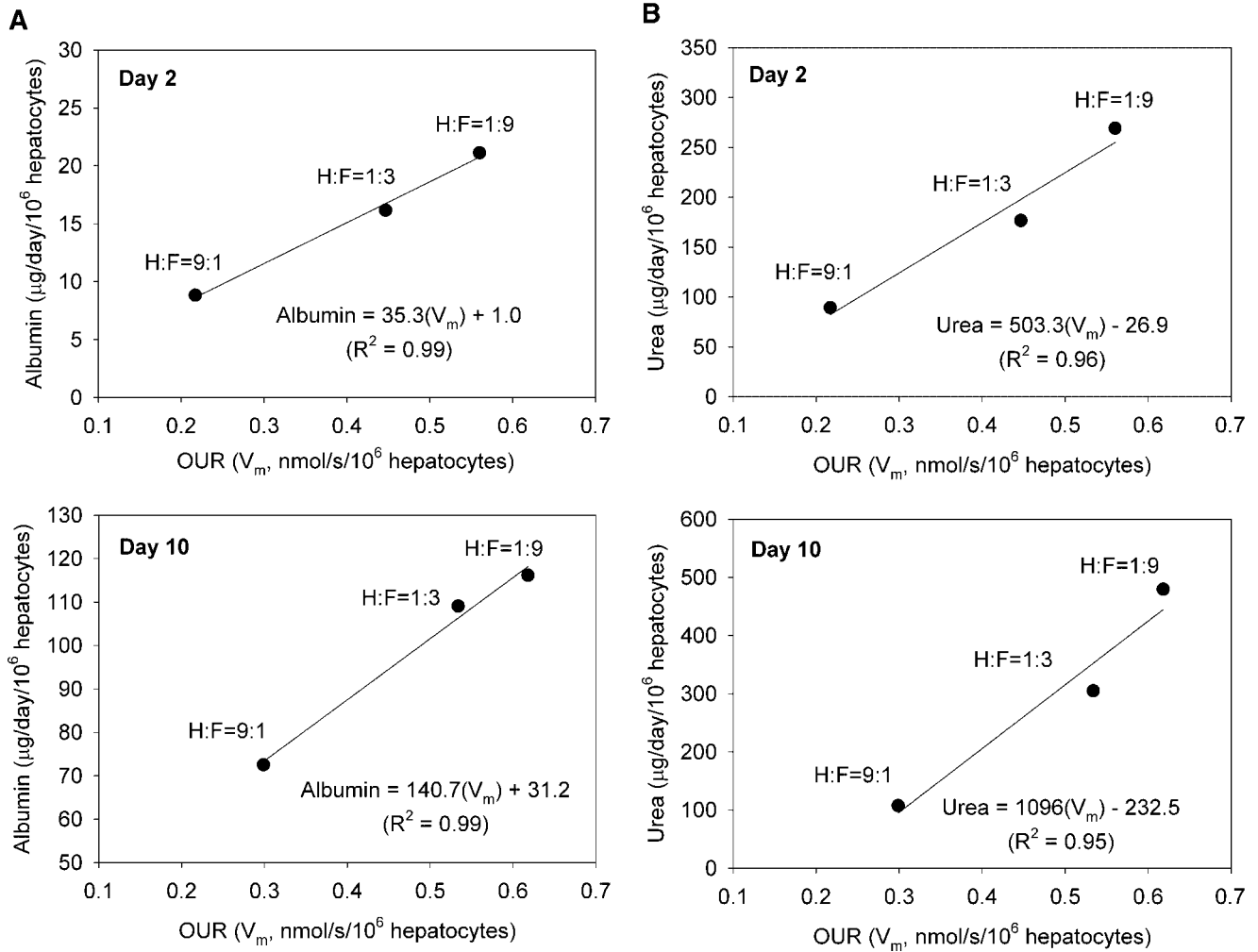


Figure 7. Correlation between OURs (V_m) and liver-specific functions (albumin secretion and urea synthesis) at various hepatocyte seeding densities. **A:** OUR versus albumin secretion. **B:** OUR versus urea synthesis. Upper panels show day 2 data and lower panels show day 10 data.

production with increased OUR compared to higher hepatocyte density co-cultures.

Mathematical Model Prediction of Oxygen Uptake Rates

In an effort to predict the OURs of co-cultures with different ratios of hepatocytes and fibroblasts, we developed a mathematical model using the data on OURs of co-cultures of hepatocytes and fibroblasts ($V_{m,\text{coculture}}$), OURs of hepatocytes and fibroblasts alone ($V_{m,\text{hep}}$ and $V_{m,\text{fb}}$), and the cell numbers (N_{hep} and N_{fb}). First, linear summation of OURs of individual cell types ($V_{m,\text{coculture}} = V_{m,\text{hep}}N_{\text{hep}} + V_{m,\text{fb}}N_{\text{fb}}$) was tested and compared with the experimental data measured for the co-cultures. As seen in Figure 8A, OURs determined by linear summation did not fit the data throughout the culture days and was always lower than the measured co-culture OURs. The measured

OURs for the co-cultures on day 10 were higher (71, 75, 22% at low, medium, high hepatocyte densities, respectively) than those calculated by linear summation of OURs of individual cell types. Similar trends were observed on other culture days. This suggested that in the co-culture system, there might be a synergistic effect on hepatocyte metabolism by heterotypic cell–cell interactions between the cultured hepatocytes and fibroblasts. Hence, we adapted a nonlinear Michaelis–Menten model for OUR (V_m) in the co-culture systems (Eq. 2), and fitted the experimental data to this equation. All model parameters ($a = 1.0290$, $b = 1.3899$, $c = 0.9994$, $d = 4.7173$, $e = 1.0000$, $f = 1.0000$) were determined by constrained nonlinear optimization using MATLAB. Using the cell numbers, model parameters, and OURs of hepatocytes and fibroblasts alone, the mathematical model was used to predict the experimental data measured in the co-culture system. Figure 8B shows the model predictions for both training (OUR for days 2, 7, and 10 of culture) and test data (day 14) obtained after

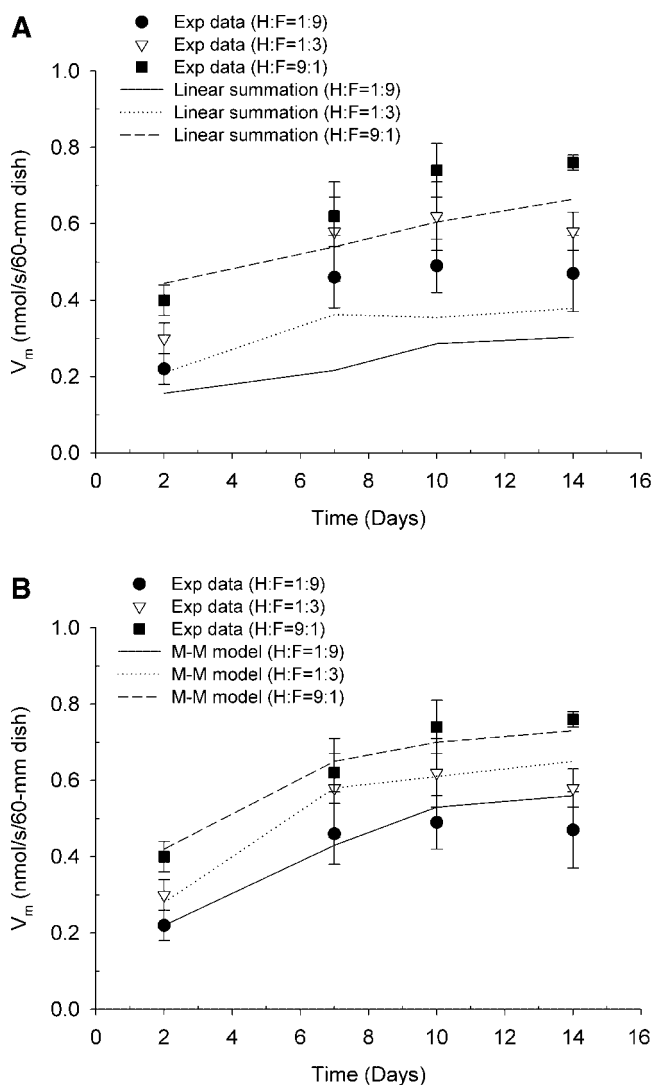


Figure 8. Linear summation and mathematical model prediction of OURs over time. **A:** Linear summation, **B:** nonlinear Michaelis–Menten (M–M) model. OUR values used for $V_{m,hep}$ and $V_{m,fb}$ in linear summation and the model prediction were 0.24 and 0.06 (nmol/s/ 10^6 cells), respectively. Linear summation for co-culture is the sum of OURs of individual cell types ($V_{m,coculture} = V_{m,hep}N_{hep} + V_{m,fb}N_{fb}$). For the Michaelis–Menten model (Eq. 2), model parameters calculated by constrained nonlinear optimization using MATLAB. The symbols show experimental data and the lines indicate linear summation and model predictions. Experimental data shown are means \pm standard deviations of three independent experiments ($n=3-5$).

optimizing Equation 2 as explained in Methods section. As can be seen, model predictions were close to experimental data for both the training and test data sets (Fig. 8B).

Discussion

Hepatocytes are highly metabolic with high OUR. In static culture conditions, hepatocytes may easily become hypoxic due to the low solubility and limited diffusion of oxygen in

aqueous media, a problem that is exacerbated in high hepatocyte density cultures. In the optimal design of BAL devices, a sufficient supply of oxygen, and other nutrients, to the hepatocytes is critical. Several studies using oxygen-permeable membranes have demonstrated their benefit in enhancing oxygen transport to the cells in these devices (De Bartolo et al., 2000; Roy et al., 2001; Tilles et al., 2001a,b). In the present study, to examine the effect of hepatocyte seeding density on OUR and liver-specific functions of hepatocytes co-cultured with 3T3-J2 fibroblasts, we varied the ratio of hepatocytes to fibroblasts while keeping the initial number of total cells seeded per dish constant. We demonstrated that lower hepatocyte density co-cultures had significantly higher OURs, and albumin and urea synthesis rates on a per hepatocyte basis than those seeded at higher densities. Increases in OUR correlated well with increased liver-specific functions.

In this study, the liver-specific functions (albumin and urea) were measured in static tissue culture conditions. The urea synthesis rates per culture dish were unaffected by the seeding density after 10 days of culture. The fact that urea synthesis levels per dish were similar for the three hepatocyte to fibroblast ratios is consistent with the possibility of oxygen limitation, and a previous report suggests that urea synthesis per cell is proportional to oxygen partial pressure at the cell surface (Bhatia et al., 1996). In cultured hepatocytes, mitochondrial activity and urea synthesis are both dependent on the oxygen concentration in the medium (Jones, 1984; Kashiwagura et al., 1984). Schumacker et al. (1993) reported that hepatocytes are capable of reversibly reducing their metabolic activity and oxygen consumption in response to reduced oxygen tension. In the case of albumin secretion, prior studies suggest that albumin secretion is not affected by the oxygen tension. Thus, it is less likely that oxygen transport limitations play a role in the higher albumin secretion per cell seen at lower hepatocyte to fibroblast ratios. Other factors, such as the greater extent of heterotypic cellular interactions at the lower hepatocyte to fibroblast ratios could be involved (Bhatia et al., 1998). In contrast to the measurement of liver-specific functions, the OURs were measured under well-mixed conditions and represent the maximum oxygen uptake capacity of the cells. During the measurement of OURs, the oxygen tension as a function of time decreased linearly down to ~ 15 mmHg ($\sim 2\%$ oxygen). The OURs were based on the linear portion of the curve, where no oxygen limitation occurs. The higher OUR per cell at lower hepatocyte to fibroblast ratios, therefore, represents an intrinsic difference in hepatocyte metabolism. These results are consistent with previous reports (Custer and Mullon, 1998; Patzer, 2004; Sand et al., 1977; Sielaff et al., 1997), which showed that increasing hepatocyte cell density decreases OUR of hepatocytes. It is likely that this difference also contributes to the differences in albumin and urea secretion mentioned above, but has not been investigated yet.

Hepatocytes are known to consume more oxygen in the early phase of culture (days 0–1) when attachment and

spreading occur, and tend to consume less oxygen (~40%) at later time points in stable long-term cultures in collagen sandwich configuration (Foy et al., 1994; Rotem et al., 1992; Yarmush et al., 1992). The results herein are consistent with these prior observations. Pure hepatocyte cultures (used as controls) exhibited relatively high OUR in the early phase of culture (day 1) and decreased by approximately 27% in the stable long-term culture in collagen gel sandwich (day 14). On a per cell basis, high hepatocyte densities (H:F = 9:1) in long-term co-cultures had almost the same OUR (~0.24 nmol/s/10⁶ hepatocytes) as that of pure hepatocyte cultures in collagen gel sandwich configuration. However, lower hepatocyte density co-cultures demonstrated significantly higher OURs and liver-specific functions on a per hepatocyte basis than those seeded at higher densities. Values determined early in the culture (day 2), at which point cell numbers were close to initial seeding densities, also demonstrated that hepatocytes maintained higher levels of functions and consumed more oxygen at low hepatocyte densities than at high hepatocyte densities.

In this study, we took into account the proliferation of hepatocytes and fibroblasts in co-cultures to determine OURs and liver-specific functions on a per hepatocyte basis. It is well known that primary hepatocytes have low mitotic activity *in vitro*; however, our data suggest that hepatocytes co-cultured with fibroblasts (3T3-J2) exhibit a measurable proliferative activity. This finding is consistent with previous reports which have demonstrated that hepatocytes co-cultured with various types of nonparenchymal cells can proliferate (Mizuguchi et al., 2001; Shimaoka et al., 1987; Uyama et al., 2002). Lower hepatocyte density co-cultures demonstrated greater hepatocyte proliferation than those at higher densities. Hepatocyte numbers (determined by nuclear counting) in high, medium, and low hepatocyte density cultures increased by approximately 1.4-, 2-, and 3-fold over 14 days, respectively. Previous reports have also mentioned that hepatocyte proliferation was greater in co-cultures seeded at lower hepatocyte densities (Corlu et al., 1997; Nakamura et al., 1983; Shimaoka et al., 1987). A potential explanation for this is that fibroblasts produce growth factors and insoluble molecules for hepatocytes and vice-versa (Gressner et al., 1993; Matsumoto et al., 1992; Mizuguchi et al., 2001; Schmidtchen et al., 1990; Skrtic et al., 2000; Story, 1989). Thus, it is expected that large numbers of fibroblasts favor hepatocyte proliferation while large numbers of hepatocytes favor fibroblast proliferation. Conversely, fibroblasts and hepatocytes may inhibit their own growth at high densities due to secreted factors or contact inhibition of growth. A report describing hepatocyte proliferation in the co-culture system will be published as a separate article.

We developed a mathematical model to predict OUR in the co-culture system and to investigate the correlation between OUR of hepatocytes cultured alone and OUR of co-cultured hepatocytes. OUR calculated by linear summation using OURs of monocultures of hepatocytes and fibroblasts, and accounting for cell numbers, were not in

good agreement with the experimental data and were always lower than the measured OUR for the co-cultures. When the measured OURs were modeled using Michaelis–Menten kinetics, model predictions of OUR closely correlated with the experimental data. The model predicted OUR within the experimental data set (interpolation) as well as outside the data set range (extrapolation). In the model, the parameters *a–f* indicate the influence of OUR for a particular cell type (in this case either hepatocytes or fibroblasts) on the total OUR in co-culture. Essentially, the parameters decrease or increase the effective contributions to the total OUR. Each parameter adds weight to the effective OUR ($V_{m,j}N_j$), in terms of the *j*th component. Only parameter values close to zero have no significance. The proposed model can in principle predict OURs for various co-cultured cell types and seeding ratios. Although the model shown earlier is for two cell types, it can be easily adapted for co-culture systems with multiple cell types as

$$\text{OUR}(V_{m,\text{coculture}}) = \sum_{j=1}^n \left(\frac{b_j V_{m,j} N_j t}{1 + \sum_{i=1}^n b_{i,j} V_{m,i} N_i t} \right) \quad (3)$$

The necessity of the nonlinear formulation of OUR is based on the fact that in the co-culture system, there is a synergistic effect on hepatocyte metabolism from nonparenchymal cells such as fibroblasts. The presented model can innately capture the nonlinear contribution due to proliferating cells, as well as the co-culture effect of various cell types on one or many cells.

This study provides useful information for the design of BAL devices. For example, in designing a clinically scaled BAL device, the goal would be to maximize the liver-specific functions per surface area available within the device. It is estimated that approximately 10% of the liver mass is necessary to support a patient with acute liver failure, which corresponds to a device containing approximately 10¹⁰ hepatocytes, a cell seeding surface area of 10 m² (i.e., 10⁵ cells/cm²), and a priming volume of 1 L. The results obtained in this study indicate that cultures with low hepatocyte to fibroblast ratios (H:F = 1:9) had the highest albumin secretion rates on a per hepatocyte basis, whereas the cultures with high hepatocyte to fibroblast ratios (H:F = 9:1) secreted, in general, the most albumin on a per surface area basis. In order to obtain equivalent albumin secretion rates, cultures with a H:F = 1:9 would need a surface area 2.7 times greater than that of cultures with a H:F = 9:1. Using a flat-plate design, this larger surface area requirement would directly translate into a BAL device with a priming volume 2.7 times greater than that for a device cultured with a H:F = 9:1, which would far exceed the ideal maximum of 1 L. In contrast to albumin secretion rates, urea synthesis rates when calculated on a surface area basis were equivalent for all three H:F ratios tested on days 10 and 14. This result is consistent with the possibility of oxygen

limitations occurring at higher hepatocyte to fibroblast ratios. Knowing this information is critical in designing BAL devices that will avoid oxygen limitations, as well as maximize liver-specific functions.

In summary, this study evaluated oxygen consumption characteristics and liver-specific functions of hepatocytes in co-culture with 3T3-J2 fibroblasts at various hepatocyte to fibroblast seeding ratios. Lower hepatocyte density co-cultures had significantly higher OURs and liver-specific functions on a per hepatocyte basis than those seeded at higher hepatocyte densities. Increases in OUR correlated with increased liver-specific functions. We also modeled OUR by fitting Michaelis–Menten kinetics and the model predictions closely correlated with the experimental data. This study provides information that is useful for the design of efficient BAL devices.

References

- Balis UJ, Behnia K, Dwarakanath B, Bhatia SN, Sullivan SJ, Yarmush ML, Toner M. 1999. Oxygen consumption characteristics of porcine hepatocytes. *Metab Eng* 1(1):49–62.
- Berthiaume F, Moghe PV, Toner M, Yarmush ML. 1996. Effect of extracellular matrix topology on cell structure, function, and physiological responsiveness: Hepatocytes cultured in a sandwich configuration. *FASEB J* 10(13):1471–1484.
- Bhatia SN, Toner M, Foy BD, Rotem A, O'Neil KM, Tompkins RG, Yarmush ML. 1996. Zonal Liver Cell Heterogeneity: Effects of Oxygen on Metabolic Functions of Hepatocytes. *J Cell Eng* 1:125–135.
- Bhatia SN, Balis UJ, Yarmush ML, Toner M. 1998. Microfabrication of hepatocyte/fibroblast co-cultures: Role of homotypic cell interactions. *Biotechnol Prog* 14(3):378–387.
- Bhatia SN, Balis UJ, Yarmush ML, Toner M. 1999. Effect of cell-cell interactions in preservation of cellular phenotype: Cocultivation of hepatocytes and nonparenchymal cells. *FASEB J* 13(14):1883–1900.
- Catapano G. 1996. Mass transfer limitations to the performance of membrane bioartificial liver support devices. *Int J Artif Organs* 19(1):18–35.
- Corlu A, Ilyin G, Cariou S, Lamy I, Loyer P, Guguen-Guillouzo C. 1997. The coculture: A system for studying the regulation of liver differentiation/proliferation activity and its control. *Cell Biol Toxicol* 13(4-5):235–242.
- Custer L, Mullon CJ. 1998. Oxygen delivery to and use by primary porcine hepatocytes in the HepatAssist 2000 system for extracorporeal treatment of patients in end-stage liver failure. *Adv Exp Med Biol* 454:261–271.
- De Bartolo L, Jarosch-Von Schweder G, Haverich A, Bader A. 2000. A novel full-scale flat membrane bioreactor utilizing porcine hepatocytes: Cell viability and tissue-specific functions. *Biotechnol Prog* 16(1):102–108.
- Demetriou AA, Brown RS, Jr., Busuttill RW, Fair J, McGuire BM, Rosenthal P, Am Esch JS, II, Lerut J, Nyberg SL, Salizzoni M, et al. 2004. Prospective, randomized, multicenter, controlled trial of a bioartificial liver in treating acute liver failure. *Ann Surg* 239(5):660–667; discussion 667–670.
- Dunn JC, Yarmush ML, Koebe HG, Tompkins RG. 1989. Hepatocyte function and extracellular matrix geometry: Long-term culture in a sandwich configuration. *FASEB J* 3(2):174–177.
- Dunn JC, Tompkins RG, Yarmush ML. 1991. Long-term in vitro function of adult hepatocytes in a collagen sandwich configuration. *Biotechnol Prog* 7(3):237–245.
- Dunn JC, Tompkins RG, Yarmush ML. 1992. Hepatocytes in collagen sandwich: Evidence for transcriptional and translational regulation. *J Cell Biol* 116(4):1043–1053.
- Ellis AJ, Hughes RD, Wendon JA, Dunne J, Langley PG, Kelly JH, Gislason GT, Sussman NL, Williams R. 1996. Pilot-controlled trial of the extracorporeal liver assist device in acute liver failure. *Hepatology* 24(6):1446–1451.
- Foy BD, Rotem A, Toner M, Tompkins RG, Yarmush ML. 1994. A device to measure the oxygen uptake rate of attached cells: Importance in bioartificial organ design. *Cell Transplant* 3(6):515–527.
- Fraslin JM, Kneip B, Vaulont S, Glaise D, Munnich A, Guguen-Guillouzo C. 1985. Dependence of hepatocyte-specific gene expression on cell-cell interactions in primary culture. *EMBO J* 4(10):2487–2491.
- Gressner AM, Brenzel A, Vossmeier T. 1993. Hepatocyte-conditioned medium potentiates insulin-like growth factor (IGF) 1 and 2 stimulated DNA synthesis of cultured fat storing cells. *Liver* 13(2):86–94.
- Guguen-Guillouzo C, Clement B, Baffet G, Beaumont C, Morel-Chany E, Glaise D, Guillouzo A. 1983. Maintenance and reversibility of active albumin secretion by adult rat hepatocytes co-cultured with another liver epithelial cell type. *Exp Cell Res* 143(1):47–54.
- Hay PD, Veitch AR, Smith MD, Cousins RB, Gaylor JD. 2000. Oxygen transfer in a diffusion-limited hollow fiber bioartificial liver. *Artif Organs* 24(4):278–288.
- Jones DP. 1984. Effect of mitochondrial clustering on O₂ supply in hepatocytes. *Am J Physiol* 247(1 Pt 1):C83–C89.
- Kashiwagura T, Wilson DF, Erecinska M. 1984. Oxygen dependence of cellular metabolism: The effect of O₂ tension on gluconeogenesis and urea synthesis in isolated rat hepatocytes. *J Cell Physiol* 120(1):13–18.
- Krihak MK, Shahriari MR. 1996. All solid state fiber optic oxygen sensor based on the sol-gel coating technique. *Electron Lett* 32:240.
- Matsumoto K, Okazaki H, Nakamura T. 1992. Up-regulation of hepatocyte growth factor gene expression by interleukin-1 in human skin fibroblasts. *Biochem Biophys Res Commun* 188(1):235–243.
- Mesnil M, Fraslin JM, Piccoli C, Yamasaki H, Guguen-Guillouzo C. 1987. Cell contact but not junctional communication (dye coupling) with biliary epithelial cells is required for hepatocytes to maintain differentiated functions. *Exp Cell Res* 173(2):524–533.
- Mizuguchi T, Hui T, Palm K, Sugiyama N, Mitaka T, Demetriou AA, Rozga J. 2001. Enhanced proliferation and differentiation of rat hepatocytes cultured with bone marrow stromal cells. *J Cell Physiol* 189(1):106–119.
- Nakamura T, Tomita Y, Ichihara A. 1983. Density-dependent growth control of adult rat hepatocytes in primary culture. *J Biochem (Tokyo)* 94(4):1029–1035.
- Nyberg SL, Shirabe K, Peshwa MV, Sielaff TD, Crotty PL, Mann HJ, Rimmel RP, Payne WD, Hu WS, Cerra FB. 1993. Extracorporeal application of a gel-entrapment, bioartificial liver: Demonstration of drug metabolism and other biochemical functions. *Cell Transplant* 2(6):441–452.
- Nyberg SL, Rimmel RP, Mann HJ, Peshwa MV, Hu WS, Cerra FB. 1994. Primary hepatocytes outperform Hep G2 cells as the source of biotransformation functions in a bioartificial liver. *Ann Surg* 220(1):59–67.
- Park J, Berthiaume F, Toner M, Yarmush ML, Tilles AW. 2005. Micro-fabricated grooved substrates as platforms for bioartificial liver reactors. *Biotechnol Bioeng* 90(5):632–644.
- Patzer JF, II. 2004. Oxygen consumption in a hollow fiber bioartificial liver—Revisited. *Artif Organs* 28(1):83–98.
- Peng CA, Palsson BO. 1996. Determination of specific oxygen uptake rates in human hematopoietic cultures and implications for bioreactor design. *Ann Biomed Eng* 24(3):373–381.
- Rotem A, Toner M, Tompkins RG, Yarmush ML. 1992. Oxygen uptake rates in cultured rat hepatocytes. *Biotechnol Bioeng* 40:1286–1291.
- Roy P, Baskaran H, Tilles AW, Yarmush ML, Toner M. 2001. Analysis of oxygen transport to hepatocytes in a flat-plate microchannel bioreactor. *Ann Biomed Eng* 29(11):947–955.
- Sand T, Condie R, Rosenberg A. 1977. Metabolic crowding effect in suspension of cultured lymphocytes. *Blood* 50(2):337–346.
- Schmidtchen A, Carlstedt I, Malmstrom A, Fransson LA. 1990. Inventory of human skin fibroblast proteoglycans. Identification of multiple heparan and chondroitin/dermatan sulphate proteoglycans. *Biochem J* 265(1):289–300.

- Schumacker PT, Chandel N, Agusti AG. 1993. Oxygen conformance of cellular respiration in hepatocytes. *Am J Physiol* 265(4 Pt 1):L395–L402.
- Seglen PO. 1976. Preparation of isolated rat liver cells. *Methods Cell Biol* 13:29–83.
- Shatford RA, Nyberg SL, Meier SJ, White JG, Payne WD, Hu WS, Cerra FB. 1992. Hepatocyte function in a hollow fiber bioreactor: A potential bioartificial liver. *J Surg Res* 53(6):549–557.
- Shimaoka S, Nakamura T, Ichihara A. 1987. Stimulation of growth of primary cultured adult rat hepatocytes without growth factors by coculture with nonparenchymal liver cells. *Exp Cell Res* 172(1):228–242.
- Shito M, Tilles AW, Tompkins RG, Yarmush ML, Toner M. 2003. Efficacy of an extracorporeal flat-plate bioartificial liver in treating fulminant hepatic failure. *J Surg Res* 111(1):53–62.
- Sielaff TD, Nyberg SL, Rollins MD, Hu MY, Amiot B, Lee A, Wu FJ, Hu WS, Cerra FB. 1997. Characterization of the three-compartment gel-entrapment porcine hepatocyte bioartificial liver. *Cell Biol Toxicol* 13(4-5):357–364.
- Skrtec S, Wallenius K, Gressner AM, Jansson JO. 2000. Characterization of hepatocyte-derived mitogenic activity on hepatic stellate cells. *Liver* 20(2):157–164.
- Smith MD, Smirthwaite AD, Cairns DE, Cousins RB, Gaylor JD. 1996. Techniques for measurement of oxygen consumption rates of hepatocytes during attachment and post-attachment. *Int J Artif Organs* 19(1):36–44.
- Story MT. 1989. Cultured human foreskin fibroblasts produce a factor that stimulates their growth with properties similar to basic fibroblast growth factor. *In Vitro Cell Dev Biol* 25(5):402–408.
- Tilles A, Balis U, Baskaran H, Yarmush M, Toner M. 2001a. Internal membrane oxygenation removes substrate oxygen limitations in a small-scale flat-plate hepatocyte bioreactor. In: Ikada Y, Ohshima N, editors. *Tissue Engineering for Therapeutic Use 5*. Amsterdam: Elsevier.
- Tilles AW, Baskaran H, Roy P, Yarmush ML, Toner M. 2001b. Effects of oxygenation and flow on the viability and function of rat hepatocytes cocultured in a microchannel flat-plate bioreactor. *Biotechnol Bioeng* 73(5):379–389.
- Uyama N, Shimahara Y, Kawada N, Seki S, Okuyama H, Iimuro Y, Yamaoka Y. 2002. Regulation of cultured rat hepatocyte proliferation by stellate cells. *J Hepatol* 36(5):590–599.
- Yarmush ML, Toner M, Dunn JC, Rotem A, Hubel A, Tompkins RG. 1992. Hepatic tissue engineering. Development of critical technologies. *Ann N Y Acad Sci* 665:238–252.